APPENDIX

Appendix Figure S1

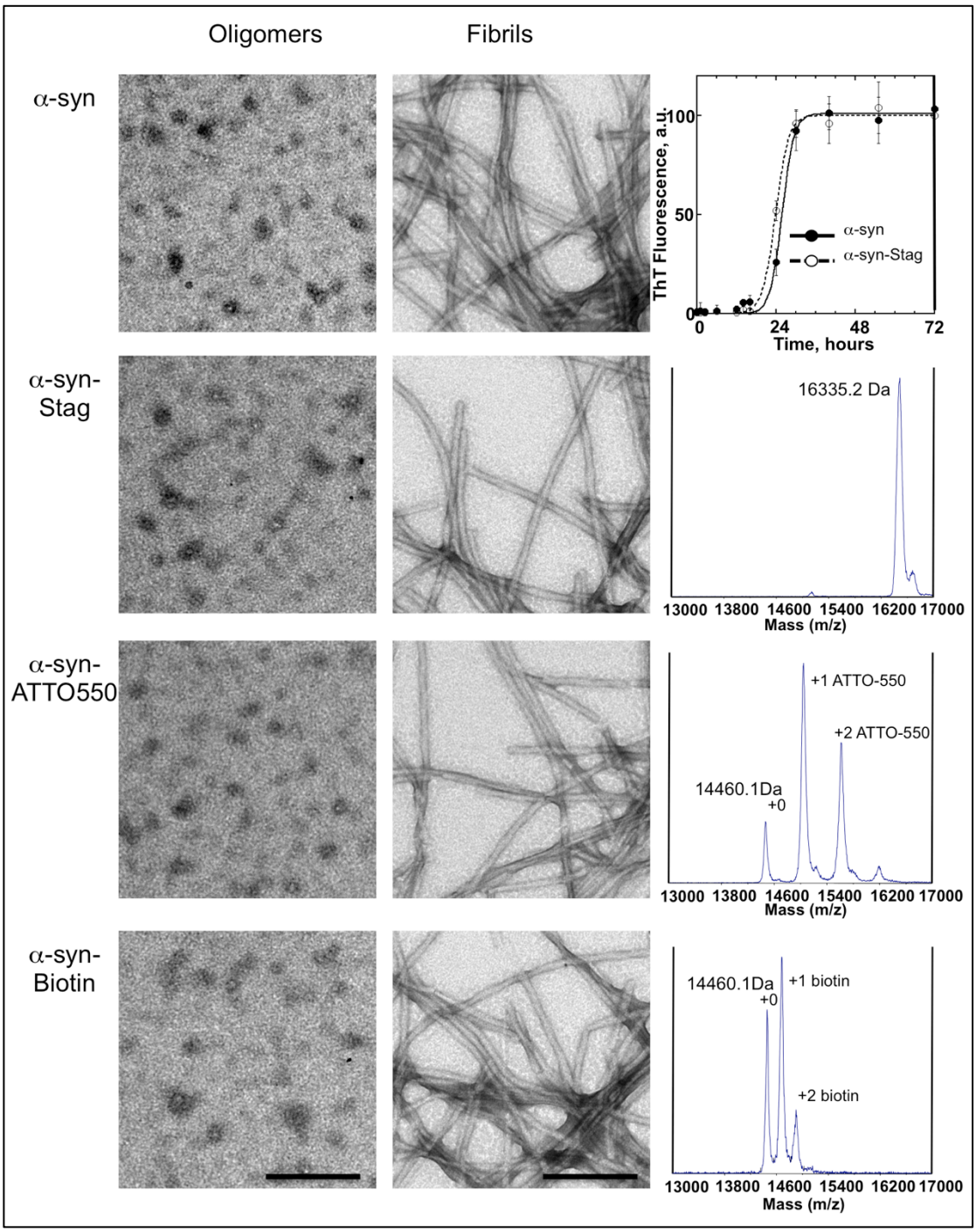

Appendix Figure S1. Characterization of α-syn assemblies used throughout this work

Electron micrographs of oligomeric (left column) and fibrillar (middle column) untagged, S-tagged, ATTO550- and biotin-labeled wild-type α-syn used throughout this study. The scale bar represents 200 nm. The assembly kinetics assessed by Thioflavin T binding of wild-type untagged (closed circle and solid line) and S-tagged-α-syn (open circles and dashed line), 100 μM, in 50 mM Tris pH 7.5, 150 mM KCl, are compared in the top panel of the column on the right. The values are mean ± S.E.M. obtained from three independent assembly reactions. No statistically significant difference is observed. The MALDI-TOF mass spectra, from top to bottom of S-tagged, ATTO-550- and biotin-labeled wild-type α-syn are shown. The spectra show that α-syn is labeled on average by one ATTO-550 or one biotin molecule.

Appendix Figure S2

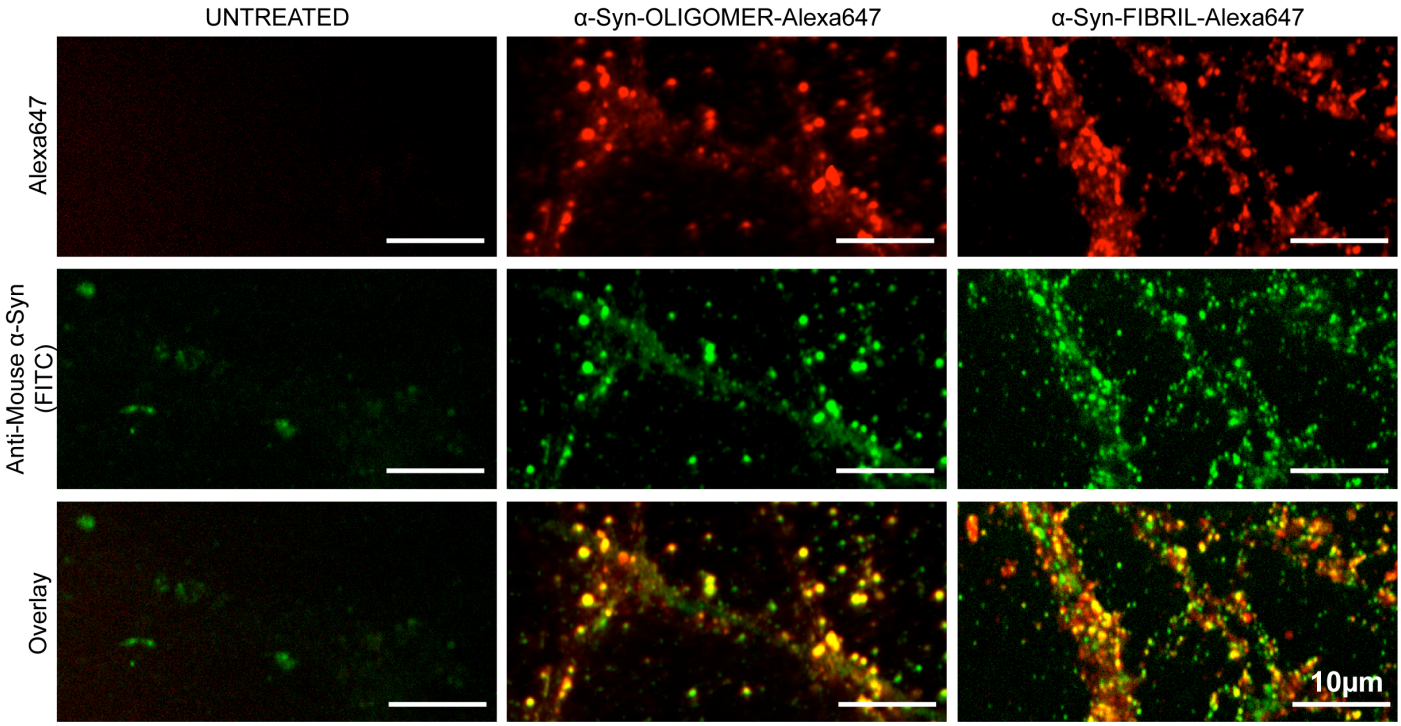

Appendix Figure S2. Immunodetection of α-syn clusters on cell surface

Cultured striatal neurons unexposed or exposed (60 min) to alexa647-labeled oligomeric (25 nM) or fibrillar (0.03 nM) α-syn (red) followed by immunolabeling using α-syn antibody (green) without permeabilization. Almost all alexa647-α-syn clusters were also immunoreactive indicating cell surface localization.

Appendix Figure S3

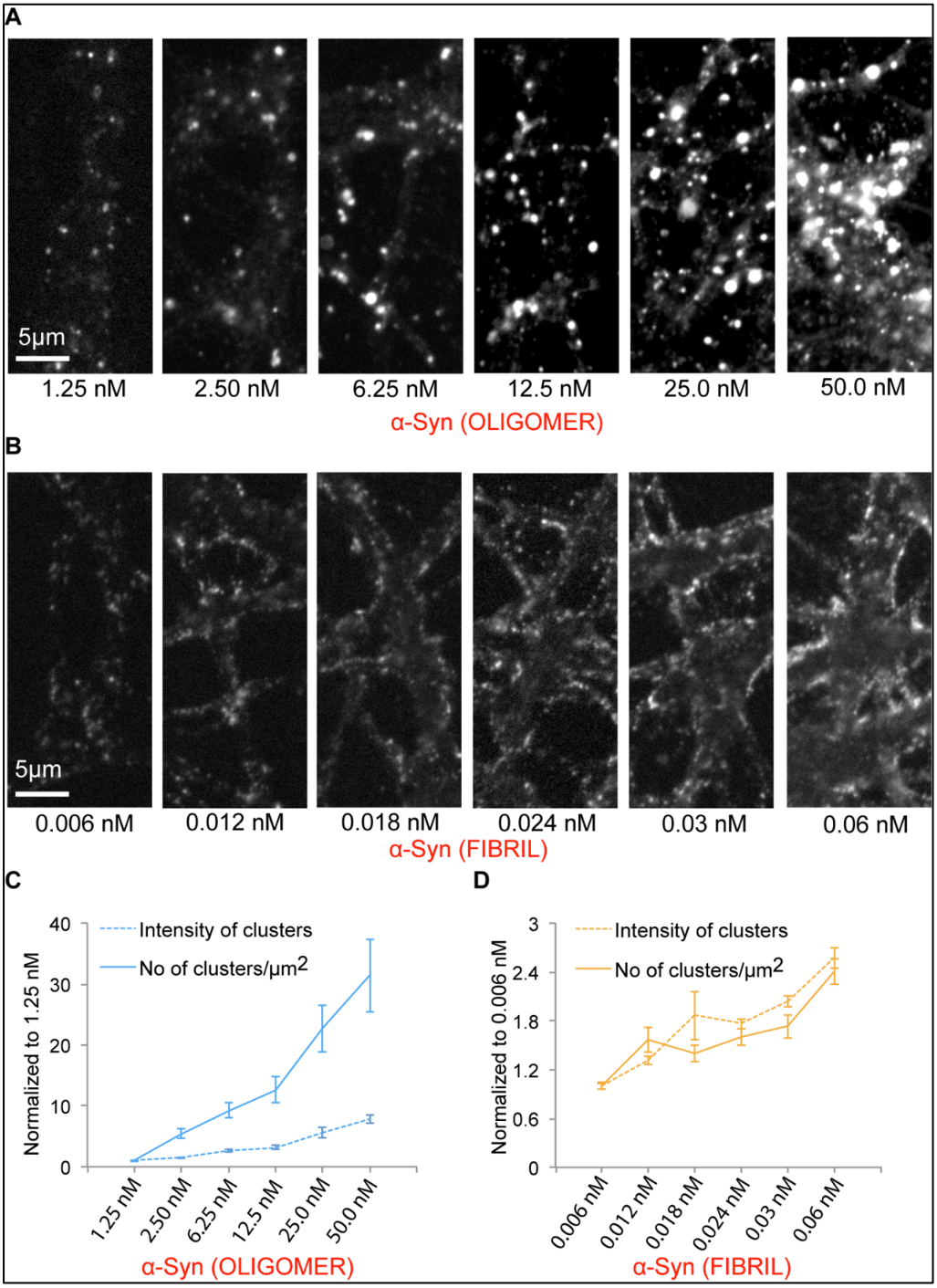

Appendix Figure S3. Concentration-dependent increase in α-syn clustering

(**A-D**) 21 DIV neurons exposed for 1 h to ATTO-550-labeled oligomeric (**A, C,** blue) or fibrillar (**B, D**, orange) α-syn at indicated concentrations. Note the concentration-dependent increase in the average fluorescence intensity and number per µm^2 of α-syn clusters. (See **Appendix Table S2** for actual values).

Appendix Figure S4

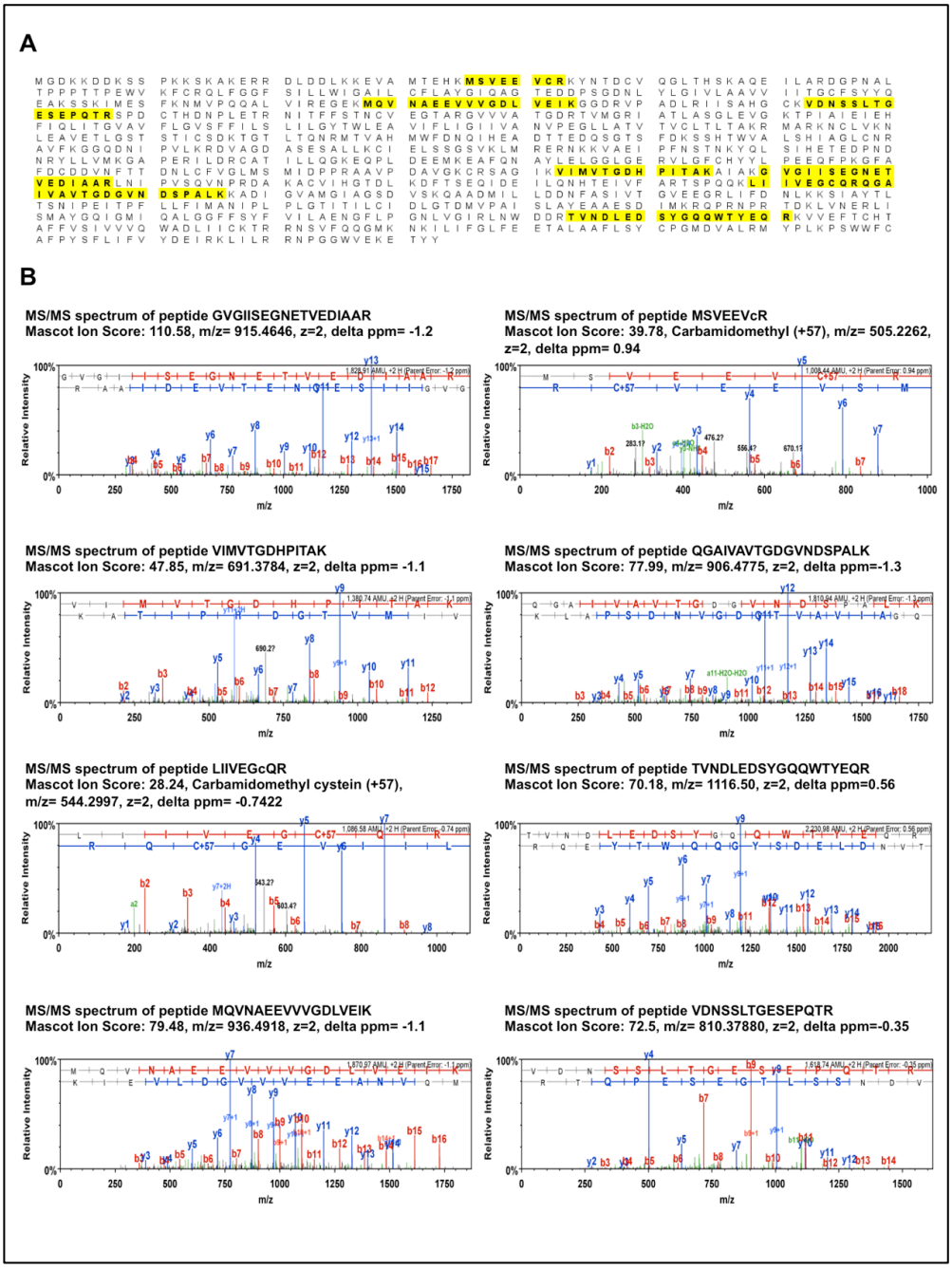

Appendix Figure S4. Example of unambiguous mass spectrometric identification of α3-NKA obtained from neurons exposed for 10 min to fibrillar α-syn

(A) Primary structure coverage of α3-NKA (Swiss Prot accession number P06687) obtained following on-beads tryptic digestion of the proteins pulled down as described in the material and methods section. The eight amino acid stretches spreads throughout the primary structure, from the N- to the C-terminus, labeled in yellow correspond to peptides identified by nanoLC-MS/MS analysis. α3-NKA is identified with confidence. The eight peptides cover 12% (117 out of 1030 amino acid residues) of α3-NKA primary structure.

(B) The MS/MS fragmentation spectra of the eight identified peptides are shown as is their primary structure, their mascot ion score and the m/z and the mass accuracy of the fragmented precursor peptide. The primary structure is determined from the y (blue) and b (red) fragment ions.

Appendix Figure S5

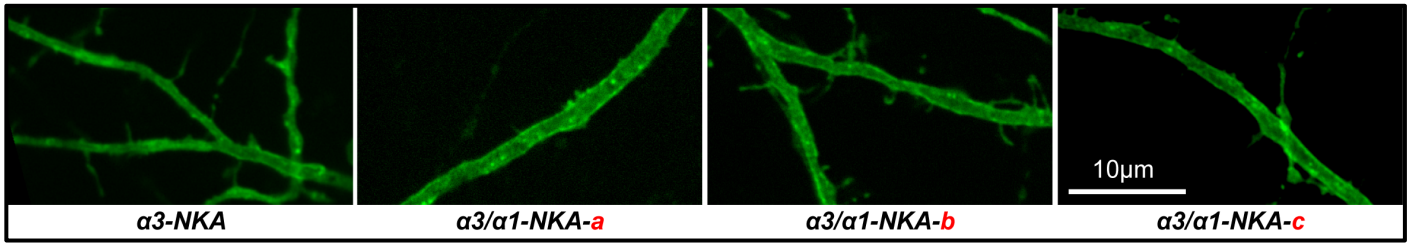

Appendix Figure S5. Membrane expression of α3-NKA and chimeric α3/α1-NKA constructs.
Neurons transfected with non-chimeric α3-NKA-pHluorin or chimeric α3/α1-NKA-pHluorin (used in **Figure 5A**). Representative images show membrane expression of chimeric constructs similar to that of the α3-NKA-pHluorin. Scale: 10 µm.

Appendix Figure S6

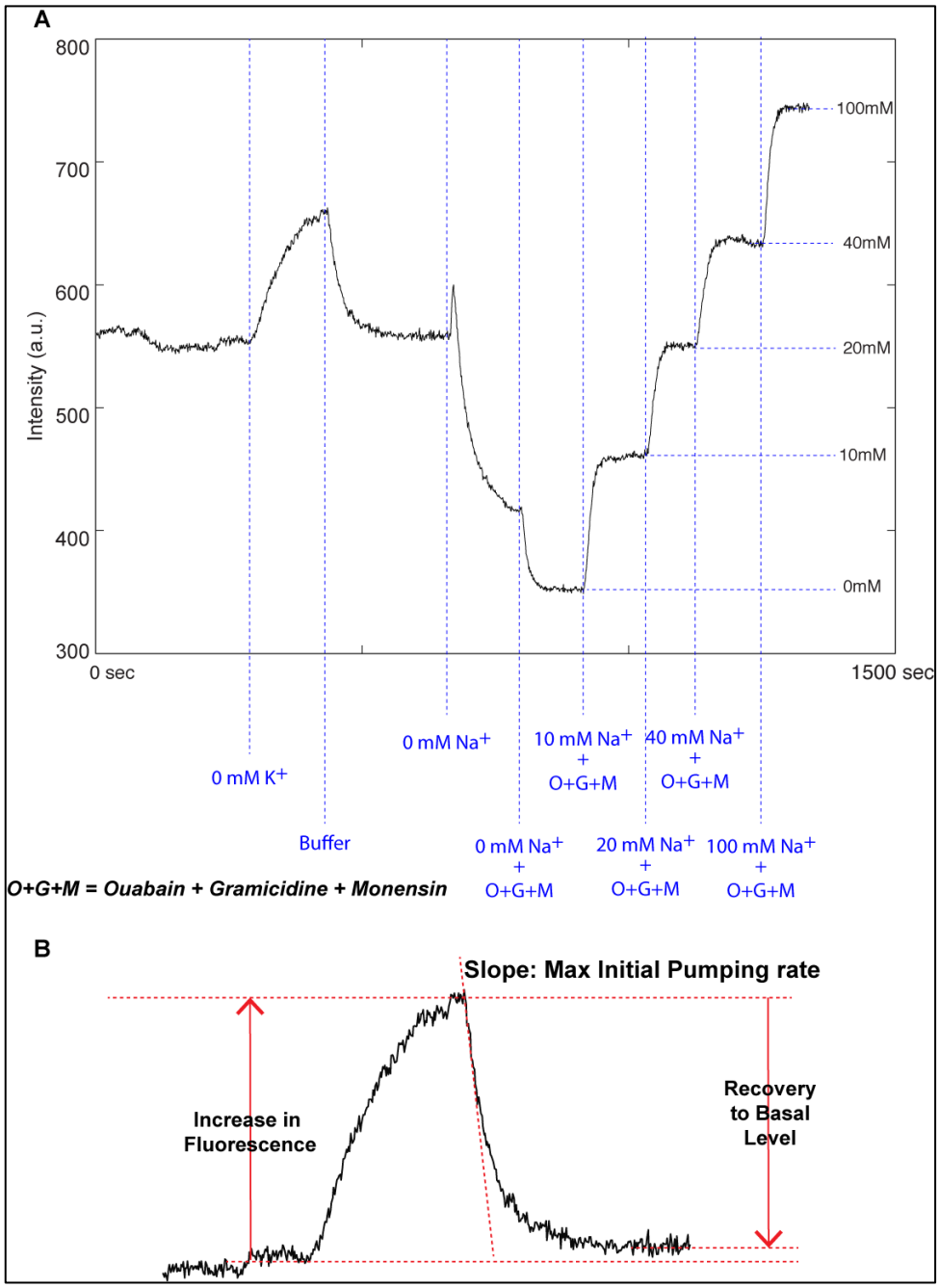

Appendix Figure S6. Protocol for the measurement of Na^+ dynamics in neurons

(**A**) A representative trace showing changes in the fluorescence intensity (Y-axis) of Na^+ dye ANG-2 following exchange of solutions as indicated in blue (See Material and Methods for all buffer compositions). First ~10 ml of 0 mM K^+ recording solution is added to increase Na^+ level in neurons. Then 0 mM K^+ recording solution is replaced with normal recording solution to visualize and measure the extrusion/efflux of Na^+ ions. This step is followed by step-wise Na^+ calibration as illustrated.

(**B**) Figure showing different parameters computed and plotted in **Figure 9B-D** and **Figure EV4**. Increases in fluorescence measure the relative rise in ANG-2 fluorescence following 0 mM K^+ recording solution application. The initial slope of decay curve measures the "Max Initial Pumping Rate". Recovery to basal level measures the difference between recovered Na^+ level and basal level.

Appendix Table S1

(Data used in Figure 1B)

Age-Dependent Clustering of α-Syn Assemblies

Oligomeric α-syn		
	Intensity of Clusters (Normalized to DIV 7) (Mean ± SEM)	
DIV 7	1.00 ± 0.03 (n=20)	
DIV 14	1.23 ± 0.07 (n=24) (**)	} (***)
DIV 21	2.35 ± 0.13 (n=35) (***)	
Fibrillar α-syn		
DIV 7	1.00 ± 0.03 (n=41)	
DIV 14	1.29 ± 0.03 (n=30) (***)	} (ns)
DIV 21	1.26 ± 0.04 (n=28) (***)	

t-test to compare difference between DIV 7 and DIV 14/21 or DIV 14 and DIV 21

ns = not significant, * $p<0.05$; ** $p<0.01$; *** $p<0.001$

n = field of view (3-experiments on three independent cultures)

Appendix Table S2

(Data supporting Figure S3)

Concentration-Dependent Clustering of α-Syn Assemblies

	Intensity of Clusters (Normalized to lowest conc.) (Mean ± SEM)	**No. of Clusters/μm^2** (Normalized to lowest conc.) (Mean ± SEM)
Oligomeric α-syn		
1.25 nM	1.00 ± 0.08 (n=20)	1.00 ± 0.12 (n=20)
2.50 nM	1.51 ± 0.10 (n=20) (ns)	5.37 ± 0.79 (n=20) (ns)
6.25 nM	2.63 ± 0.29 (n=20) (ns)	9.20 ± 1.25 (n=20) (ns)
12.50 nM	3.16 ± 0.30 (n=20) (**)	12.64 ± 2.12 (n=20) (*)
25.00 nM	5.56 ± 0.81(n=20) (***)	22.65 ± 3.84 (n=20) (***)
50.00 nM	7.83 ± 0.71 (n=20) (***)	31.39 ± 5.96 (n=20) (***)
Fibrillar α-syn		
0.006 nM	1.00 ± 0.04 (n=20)	1.00 ± 0.04 (n=20)
0.012 nM	1.31 ± 0.05 (n=20) (ns)	1.57 ± 0.16 (n=20) (**)
0.018 nM	1.87 ± 0.30 (n=20) (***)	1.40 ± 0.10 (n=20) (ns)
0.024 nM	1.76 ± 0.06 (n=20) (***)	1.60 ± 0.10 (n=20) (**)
0.030 nM	2.04 ± 0.07 (n=20) (***)	1.74 ± 0.15 (n=20) (***)
0.060 nM	2.57 ± 0.13 (n=10) (***)	2.41 ± 0.16 (n=10) (***)

One-way ANOVA with Dunnett's test to compare the difference from lowest concentration used (Oligomer: 1.25 nM; Fibril: 0.006 nM) (2 experiments)

ns = not significant, *p<0.05; **p<0.01; ***p<0.001

Appendix Table S3

(Data used in Figure 2A-B)

Time-Dependent Clustering of α-Syn Assemblies

Oligomeric α-syn		
	Intensity of Clusters (Normalized to 5min) (Mean ± SEM)	**No of Clusters/μm^2** (Normalized to 5min) (Mean ± SEM)
5 min	1.00 ± 0.05 (n=35)	1.00 ± 0.06 (n=35)
60 min	2.04 ± 0.14 (n=35) (***)	1.39 ± 0.06 (n=35) (***)
Fibrillar α-syn		
5 min	1.00 ± 0.02 (n=35)	1.00 ± 0.04 (n=35)
60 min	2.01 ± 0.15 (n=35) (***)	1.98 ± 0.09 (n=35) (***)

t-test to compare difference from 5min

ns = not significant, *p<0.05; **p<0.01; ***p<0.001

n = field of view; (3-experiments on three independent cultures)

Appendix Table S4

Association of α-Syn and Homer/Gephyrin

Oligomeric α-syn		
	% Association-Homer (Mean ± SEM)	**% Association-Gephyrin** (Mean ± SEM)
1.25 nM	4.8 ± 1.1 (n=20)	3.7 ± 0.8 (n=20)
2.50 nM	12.9 ± 2.1 (n=20) (ns)	11.4 ± 1.8 (n=20) (*)
6.25 nM	19.3 ± 3.3 (n=20) (***)	17.8 ± 2.8 (n=20) (***)
12.50 nM	25.5 ± 3.2 (n=20) (***)	24.8 ± 2.7 (n=20) (***)
25.00 nM	38.2 ± 2.6 (n=20) (***)	34.3 ± 1.6 (n=20) (***)
50.00 nM	45.8 ± 2.2 (n=20) (***)	45.7 ± 1.9 (n=20) (***)
Fibrillar α-syn		
0.006 nM	26.6 ± 1.4 (n=20)	23.4 ± 1.1 (n=20)
0.012 nM	36.2 ± 1.2 (n=20) (***)	33.1 ± 1.4 (n=20) (***)
0.018 nM	43.3 ± 1.9 (n=20) (***)	41.1 ± 2.3 (n=20) (***)
0.024 nM	47.5 ± 1.4 (n=20) (***)	42.3 ± 1.4 (n=20) (***)
0.030 nM	47.7 ± 0.8 (n=20) (***)	43.9 ± 1.4 (n=20) (***)
0.060 nM	60.1 ± 1.4 (n=10) (***)	59.9 ± 1.5 (n=10) (***)

One-way ANOVA with Dunnett's test to compare the difference from lowest concentration used (Oligomer: 1.25 nM; Fibril: 0.006 nM) (2 experiments)

ns = not significant, *p<0.05; **p<0.01; ***p<0.001

Appendix Table S5

List of proteins from whole neurons lysates interacting with extracellularly applied oligomeric α-syn

∞: the spectral count ratio is infinite as the protein is pulled-down only with oligomeric α-synuclein
Fold change corresponds to the average spectral count ratio of three independent replicates
In bold, the unique plasma membrane protein pulled-down both with oligomeric and fibrillar α-synuclein and presenting both transmembrane and extracellularly exposed regions.

Protein Name	Gene Name	Accession Number	Fold Change (Syn/Ctrl)
40S ribosomal protein S28	Rps28	P62858	7.0
40S ribosomal protein S5	Rps5	P24050	2.2
78 kDa glucose-regulated protein	Hspa5	P06761	5.4
AP-3 complex subunit delta-1	Ap3d1	O54774	1.8
ATP synthase subunit beta, mitochondrial	Atp5b	P10719	2.0
Calcium/calmodulin-dependent protein kinase type II subunit gamma	Camk2g	P11730	2.1
Calmodulin	Calm1	P62161	2.5
Creatine kinase B-type	Ckb	P07335	5.0
Cytoskeleton-associated protein 5	Ckap5	A2AGT5	1.7
Dihydropyrimidinase-related protein 3	Dpysl3	Q62188	2.1
Double-stranded RNA-binding protein Staufen homolog 2	Stau2	Q68SB1	1.6
Elongation factor 2	Eef2	P05197	2.0
Elongation factor Tu, mitochondrial	Tufm	P85834	5.0
ERC protein 2	Erc2	Q8K3M6	3.5
Fragile X mental retardation syndrome-related protein 1	Fxr1	Q61584	2.0
Friend of PRMT1 protein	Fop	Q9CY57	2.0
GMP synthase [glutamine-hydrolyzing]	Gmps	Q3THK7	2.0
Heterogeneous nuclear ribonucleoprotein K	Hnrnpk	P61979	1.8
Kinesin-like protein KIF2A	Kif2a	P28740	1.6
Myb-binding protein 1A	Mybbp1a	O35821	1.9
Neuron navigator 1	Nav1	Q8CH77	1.6
Non-POU domain-containing octamer-binding protein	Nono	Q5FVM4	1.7
Protein unc-13 homolog A	Unc13a	Q62768	3.5
Protein-L-isoaspartate(D-aspartate) O-methyltransferase	Pcmt1	P22062	2.5
Serine/arginine-rich splicing factor 2	Srsf2	Q62093	2.4
Serine/arginine-rich splicing factor 3	Srsf3	P84104	1.6
SLIT-ROBO Rho GTPase-activating protein 2	Srgap2	Q91Z67	2.5
Sodium/potassium-transporting ATPase subunit alpha-3	**Atp1a3**	**P06687**	**1.6**
Tubulin beta-4B chain	Tubb4b	P68372	1.6
Ubiquitin carboxyl-terminal hydrolase isozyme L1	Uchl1	Q00981	∝
Vesicle-associated membrane protein-associated protein A	Vapa	Q9WV55	4.0
WD repeat-containing protein 47	Wdr47	Q8CGF6	2.8

Appendix Table S6
List of proteins from whole neurons lysates interacting with extracellularly applied fibrillar α-syn

∞: the spectral count ratio is infinite as the protein is pulled-down only with fibrillar α-synuclein
Fold change corresponds to the average spectral count ratio of three independent replicates
In bold, the unique plasma membrane pulled-down both with oligomeric and fibrillar α-synuclein,and presenting both transmembrane and extracellularly exposed regions.
Column 5: "**Proteins identified after cross-linking**" corresponds to proteins identified after cross-linking. All the other proteins were not identified after cross-link.

Protein name	Gene name	Accession Number	Fold Change (Syn/Ctrl)	Proteins identified after cross-linking
14-3-3 protein gamma	Ywhag	P61982	∝	+
14-3-3 protein zeta/delta	Ywhaz	P63102	∝	+
40S ribosomal protein S15	RPS15	P62842	∝	+
40S ribosomal protein S16	Rps16	P14131	3.0	+
40S ribosomal protein S17	Rps17	P04644	5.0	+
40S ribosomal protein S18	Rps18	P62270	6.7	+
40S ribosomal protein S19	Rps19	P17074	∝	
40S ribosomal protein S20	Rps20	P60867	1.6	+
40S ribosomal protein S25	Rps25	P62852	13.0	
40S ribosomal protein S29	Rps29	P62274	5.5	+
40S ribosomal protein S5	Rps5	P24050	9.0	
40S ribosomal protein S7	Rps7	P62082	3.9	
5-azacytidine-induced protein 1	Azi1	Q62036	∝	
60S ribosomal protein L22-like 1	Rpl22l1	Q9D7S7	∝	
60S ribosomal protein L23	Rpl23	P62830	3.1	+
60S ribosomal protein L27	Rpl27	P61354	2.1	+
60S ribosomal protein L27a	Rpl27a	P18445	2.2	
60S ribosomal protein L38	Rpl38	P63174	∝	
Abl interactor 1	Abi1	Q8CBW3	18.0	
Acetyl-CoA acetyltransferase, mitochondrial	Acat1	P17764	∝	
Actin filament-associated protein 1	Afap1	Q8VH46	4.3	
Adenomatous polyposis coli protein	Apc	P70478	∝	
Adenomatous polyposis coli protein 2	Apc2	Q9Z1K7	∝	
ADP/ATP translocase 2	Slc25a5	P51881	3.7	
ADP-ribosylation factor GTPase-activating protein 3	Arfgap3	Q4KLN7	∝	
Agrin	Agrn	P25304	∝	
Alpha-internexin	Ina	P23565	34.0	
Alpha-tubulin N-acetyltransferase	Atat1	Q6MG11	∝	
Amphiphysin	Amph	O08838	∝	
AP-3 complex subunit beta-2	Ap3b2	Q9JME5	∝	
AP-3 complex subunit delta-1	Ap3d1	O54774	4.3	
Apolipoprotein E	Apoe	P02650	∝	
Ataxin-2	Atxn2	O70305	∝	
Ataxin-2-like protein	Atxn2l	Q7TQH0	∝	
ATP synthase subunit alpha, mitochondrial	Atp5a1	P15999	1.8	+
ATP synthase subunit d, mitochondrial	Atp5h	P31399	∝	
ATP synthase subunit gamma, mitochondrial	Atp5c1	P35435	25.0	+
ATP synthase subunit O, mitochondrial	Atp5o	Q06647	∝	
ATPase family AAA domain-containing protein 3	Atad3	Q3KRE0	∝	
ATP-dependent RNA helicase DDX3X	Ddx3x	Q62167	2.4	+
Bcl-2-associated transcription factor 1	Bclaf1	Q8K019	10.5	
Calcium-binding mitochondrial carrier protein Aralar1	Slc25a12	Q8BH59	∝	
Calmodulin-regulated spectrin-associated protein 2	Camsap2	Q8C1B1	∝	
Calmodulin-regulated spectrin-associated protein 3	Camsap3	Q80VC9	∝	
CaM kinase-like vesicle-associated protein	Camkv	Q63092	6.0	
CAP-Gly domain-containing linker protein 2	Clip2	O55156	∝	
Caskin-1	Caskin1	Q8VHK2	∝	
Catenin delta-2	Ctnnd2	O35927	∝	
Cell division control protein 42 homolog	Cdc42	P60766	∝	
Centrosomal protein of 170 kDa	Cep170	Q6A065	37.0	
Charged multivesicular body protein 2b	Chmp2b	Q8BJF9	∝	
Chromatin target of PRMT1 protein	Chtop	Q9CY57	5.3	
CLIP-associating protein 2	Clasp2	Q99JD4	1.7	
Coatomer subunit alpha	Copa	Q8CIE6	3.0	

Protein name	Gene name	Accession Number	Fold Change (Syn/Ctrl)	Proteins identified after cross-linking
Cofilin-1	Cfl1	P45592	3.8	+
Cytoplasmic dynein 1 heavy chain 1	Dync1h1	Q9JHU4	62.0	
Dihydropyrimidinase-related protein 1	Crmp1	Q62950	4.5	+
Dihydropyrimidinase-related protein 2	Dpysl2	O08553	1.6	+
Disks large-associated protein 1	Dlgap1	Q9D415	∝	
Disks large-associated protein 4	Dlgap4	P97839	∝	
DnaJ homolog subfamily A member 1	Dnaja1	P63036	∝	
DnaJ homolog subfamily B member 1	Dnajb1	Q9QYJ3	∝	
DnaJ homolog subfamily B member 2	Dnajb2	Q9QYI5	∝	
DnaJ homolog subfamily B member 5	Dnajb5	O89114	∝	
DnaJ homolog subfamily B member 6	Dnajb6	O54946	∝	
Dynactin subunit 1	Dctn1	P28023	4.0	
Elongation factor 1-alpha 1	Eef1a1	P10126	2.6	+
Elongation factor Tu, mitochondrial	Tufm	P85834	27.5	
Ena/VASP-like protein	Evl	O08719	∝	
Eukaryotic translation initiation factor 3 subunit C	Eif3c	B5DFC8	∝	
Glyceraldehyde-3-phosphate dehydrogenase	Gapdh	P04797	2.6	+
Glypican-1	Gpc1	P35053	∝	
Glypican-2	Gpc2	P51653	∝	
Glypican-4	Gpc4	P51655	∝	
Guanine nucleotide-binding protein G(I)/G(S)/G(T) subunit beta-1	Gnb1	P54311	∝	
Heat shock cognate 71 kDa protein	HSPA8	P63018	5.0	+
Hepatoma-derived growth factor-related protein 2	Hdgfrp2	Q925G1	∝	
Heterochromatin protein 1-binding protein 3	Hp1bp3	Q6P747	6.0	
Heterogeneous nuclear ribonucleoprotein D0	Hnrnpd	Q60668	∝	+
Heterogeneous nuclear ribonucleoprotein D-like	Hnrpdl	Q9Z130	∝	
Heterogeneous nuclear ribonucleoprotein K	Hnrnpk	P61979	4.5	+
Heterogeneous nuclear ribonucleoprotein M	Hnrnpm	Q62826	5.4	
Heterogeneous nuclear ribonucleoprotein U-like protein 2	Hnrnpul2	Q00PI9	2.7	+
Histone H2A.J	H2afj	A9UMV8	1.7	
Histone H2A.Z	H2afz	P0C0S6	6.0	
Histone H4	Hist1h4b	P62804	1.6	+
Host cell factor 1	Hcfc1	Q61191	∝	
IQ motif and SEC7 domain-containing protein 1	Iqsec1	Q8R0S2	∝	
Kelch-like protein 22	Klhl22	D3ZZC3	∝	
KH domain-containing, RNA-binding, signal transduction-associated protein 1	Khdrbs1	Q91V33	∝	
Kinesin heavy chain isoform 5C	Kif5c	P28738	26.5	
Lamin-B1	Lmnb1	P70615	∝	
Lipid phosphate phosphatase-related protein type 4	Lppr4	Q7TME0	∝	
Liprin-alpha-2	Ppfia2	Q8BSS9	6.0	
MAP/microtubule affinity-regulating kinase 3	Mark3	Q8VHF0	11.0	
MAP/microtubule affinity-regulating kinase 4	Mark4	Q8CIP4	∝	
MAP7 domain-containing protein 1	Map7d1	A2AJI0	∝	
Microtubule-associated protein 1B	Map1b	P14873	2.7	+
Microtubule-associated protein 1S	Map1s	P0C5W1	∝	
Microtubule-associated protein 2	Map2	P15146	5.9	+
Microtubule-associated protein 4	Map4	Q5M7W5	3.5	
Microtubule-associated protein 6	Map6	Q63560	3.0	+
Microtubule-associated protein tau	Mapt	P19332	5.4	+
Microtubule-associated serine/threonine-protein kinase 1	Mast1	Q810W7	∝	
Mitochondrial glutamate carrier 1	Slc25a22	Q9D6M3	∝	
Mitogen-activated protein kinase kinase kinase kinase 4	Map4k4	P97820	∝	
Myc box-dependent-interacting protein 1	Bin1	O08539	∝	
Myosin regulatory light chain 12B	Myl12b	P18666	∝	
Nck-associated protein 1	Nckap1	P28660	4.0	
Neurexin-1-alpha	Nrxn1	Q63372	∝	
Neurexin-2-alpha	Nrxn2	Q63374	∝	
Neurofilament light polypeptide	Nefl	P19527	∝	
Neurofilament medium polypeptide	Nefm	P12839	∝	
Neuromodulin	Gap43	P07936	4.0	+
Neuron navigator 1	Nav1	Q8CH77	44.3	

Protein name	Gene name	Accession Number	Fold Change (Syn/Ctrl)	Proteins identified after cross-linking
Neuron navigator 3	Nav3	Q80TN7	∝	
Neuronal migration protein doublecortin	Dcx	O88809	4.2	
Nucleolar and coiled-body phosphoprotein 1	Nolc1	P41777	∝	
Pinin	Pnn	O35691	∝	
Polymerase delta-interacting protein 3	Poldip3	Q8BG81	∝	
Prelamin-A/C	Lmna	P48679	∝	
Prickle-like protein 2	Prickle2	Q80Y24	∝	
Prohibitin-2	Phb2	O35129	∝	
Protein bassoon	Bsn	O88778	11.0	
Protein FAM54B	Fam54b	Q5XII9	∝	
Protein Hook homolog 3	Hook3	Q8BUK6	∝	
Protein KIAA0284	Kiaa0284	Q80U49	∝	
Protein NipSnap homolog 1	Nipsnap1	O55125	∝	
Protein piccolo	Pclo	Q9JKS6	∝	
Protein RUFY3	Rufy3	Q5FVJ0	∝	
Protein TANC2	Tanc2	A2A690	∝	
Rabphilin-3A	Rph3a	P47709	∝	
Ras GTPase-activating protein SynGAP	Syngap1	Q9QUH6	∝	
Ras-related C3 botulinum toxin substrate 1	Rac1	P63001	∝	+
Ras-related protein M-Ras	Mras	O08989	∝	
Ras-related protein Rab-8A	Rab8a	P35280	∝	
Ras-related protein Ral-A	Rala	P63322	∝	
Ras-related protein Rap-1A	Rap1a	P62835	∝	
Regulating synaptic membrane exocytosis protein 1	Rims1	Q9JIR4	1.6	
Rho GTPase-activating protein 33	Arhgap33	Q80YF9	∝	
Ribosome-binding protein 1	Rrbp1	Q99PL5	10.0	
SAFB-like transcription modulator	Sltm	Q8CH25	∝	
Septin-7	Sept7	O55131	∝	
Serine/arginine repetitive matrix protein 2	Srrm2	Q8BTI8	∝	
Serine/arginine-rich splicing factor 7	Srsf7	Q8BL97	1.8	
Serine/threonine-protein kinase DCLK1	Dclk1	Q9JLM8	2.9	
Serine/threonine-protein kinase DCLK2	Dclk2	Q5MPA9	65.0	
Serine/threonine-protein kinase MARK1	Mark1	O08678	8.0	
Serine/threonine-protein kinase MARK2	Mark2	O08679	11.0	
Signal recognition particle 54 kDa protein	Srp54	Q6AYB5	∝	
Sodium/potassium-transporting ATPase subunit alpha-3	**Atp1a3**	**P06687**	**6.0**	+
Sodium/potassium-transporting ATPase subunit beta-1	Atp1b1	P07340	2.5	
SRC kinase signaling inhibitor 1	Srcin1	Q9QXY2	3.2	
Stress-70 protein, mitochondrial	HSPA9	O35501	∝	
Synapsin-1	Syn1	P09951	29.7	
Synapsin-2	Syn2	Q63537	∝	
Synaptosomal-associated protein 47	Snap47	Q6P6S0	∝	
TBC1 domain family member 10B	Tbc1d10b	Q8BHL3	∝	
T-complex protein 1 subunit alpha	Tcp1	P11983	∝	
T-complex protein 1 subunit beta	Cct2	P80314	∝	+
T-complex protein 1 subunit delta	Cct4	P80315	∝	
T-complex protein 1 subunit gamma	Cct3	P80318	∝	
T-complex protein 1 subunit zeta	Cct6a	P80317	∝	
Testican-1	Spock1	Q62288	∝	
Thyroid hormone receptor-associated protein 3	Thrap3	Q5M7V8	∝	
Tomoregulin-1	Tmeff1	Q9QYV1	∝	
Traf2 and NCK-interacting protein kinase	Tnik	P83510	∝	
Transformer-2 protein homolog beta	Tra2b	P62996	∝	+
Transforming protein RhoA	Rhoa	P61589	∝	
Trifunctional enzyme subunit alpha, mitochondrial	Hadha	Q64428	∝	
Tropomyosin alpha-3 chain	Tpm3	Q63610	∝	
Uncharacterized protein KIAA1107	Kiaa1107	Q80TK0	∝	
Vesicle-associated membrane protein-associated protein A	Vapa	Q9WV55	∝	
Vimentin	Vim	P31000	32.5	
Voltage-dependent anion-selective channel protein 1	Vdac1	Q60932	5.0	
WD repeat-containing protein 37	Wdr37	Q8CBE3	∝	
Zinc finger CCCH domain-containing protein 18	Zc3h18	Q6TQE1	∝	
ZW10 interactor	Zwint	Q8VIL3	∝	

Appendix Table S7A

List of proteins from whole astrocytes lysates interacting with extracellularly applied oligomeric α-syn

∞: the spectral count ratio is infinite as the protein is pulled-down only with fibrillar α-synuclein
Fold change corresponds to the average spectral count ratio of three independent replicates

Protein name	Gene name	Accession Number	Fold Change (Syn/Ctrl)
14-3-3 protein epsilon	Ywhae	P62260	2.7
40S ribosomal protein S9	Rps9	P29314	1.8
60S ribosomal protein L13a	Rpl13a	P35427	1.7
60S ribosomal protein L26	Rpl26	P61255	2.7
60S ribosomal protein L7a	Rpl7a	P62425	2.2
78 kDa glucose-regulated protein	Hspa5	P06761	4.4
Alpha-enolase	Eno1	P04764	1.7
Arginyl-tRNA synthetase, cytoplasmic	Rars	P40329	∝
Aspartyl-tRNA synthetase, cytoplasmic	Dars	P15178	1.9
Bifunctional aminoacyl-tRNA synthetase	Eprs	Q8CGC7	1.6
Destrin	Dstn	Q7M0E3	7.0
Elongation factor 1-delta	Eef1d	Q68FR9	2.0
FH1/FH2 domain-containing protein 1	Fhod1	Q6P9Q4	3.0
Low-density lipoprotein receptor-related protein 2	Lrp2	P98158	6.5
Lysyl-tRNA synthetase	Kars	Q99MN1	2.2
Major vault protein	Mvp	Q62667	7.0
NHP2-like protein 1	Nhp2l1	P55770	3.0
Polyadenylate-binding protein 1	Pabpc1	Q9EPH8	4.5
Protein kinase C delta-binding protein	Prkcdbp	Q9Z1H9	2.0
Protein lin-7 homolog C	Lin7c	Q792I0	1.6
Putative ATP-dependent RNA helicase DHX30	Dhx30	Q5BJS0	2.3
Septin-2	Septin2	Q91Y81	1.7
SPATS2-like protein	Spats2l	Q5U2T3	2.2
Stress-70 protein, mitochondrial	Hspa9	P48721	2.5
Tricarboxylate transport protein, mitochondrial	Slc25a1	P32089	2.0

Table S7B

List of proteins from whole astrocytes lysates interacting with extracellularly applied fibrillar α-syn

∞: the spectral count ratio is infinite as the protein is pulled-down only with fibrillar α-synuclein

Fold change corresponds to the average spectral count ratio of three independent replicates

Protein name	Gene name	Accession Number	Fold Change (Syn/Ctrl)
ADP/ATP translocase 2	Slc25a5	P51881	2.3
Apolipoprotein E	Apoe	P02650	∝
ATP synthase subunit gamma, mitochondrial	Atp5c1	P35435	15.0
ATP synthase subunit O, mitochondrial	Atp5o	Q06647	∝
Cell division control protein 42 homolog	Cdc42	P60766	∝
Charged multivesicular body protein 2b	Chmp2b	Q8BJF9	∝
CLIP-associating protein 2	Clasp2	Q99JD4	16.0
Cofilin-1	Cfl1	P45592	2.0
78 KDa Glucose-regulated protein	Hspa5	P06761	34.0
DnaJ homolog subfamily A member 1	Dnaja1	P63036	∝
Glypican-4	Gpc4	P51655	∝
Lamin-B1	Lmnb1	P70615	∝
Pinin	Pnn	O35691	∝
Ras-related C3 botulinum toxin substrate 1	Rac1	P63001	∝
Ras-related protein Rab-8A	Rab8a	P35280	∝
Ras-related protein Ral-A	Rala	P63321	∝
Ras-related protein Rap-1A	Rap1a	P62835	∝
Vesicle-associated membrane protein-associated protein A	Vapa	Q9WV55	4.0
Voltage-dependent anion-selective channel protein 1	Vdac1	Q60932	∝
Long-chain fatty acid transport protein 1	Slc27a1	P97849	1.6
2',3'-cyclic-nucleotide 3'-phosphodiesterase	Cnp	P13233	∝
40S ribosomal protein S15	RPS15	P62842	∝
40S ribosomal protein S16	Rps16	P14131	2.2
40S ribosomal protein S17	Rps17	P04644	8.0
40S ribosomal protein S18	Rps18	P62270	6.2
40S ribosomal protein S25	Rps25	P62852	4.5
40S ribosomal protein S29	Rps29	P62274	3.0
40S ribosomal protein S7	Rps7	P62082	2.0
60S ribosomal protein L22-like 1	Rpl22l1	Q9D7S7	∝
60S ribosomal protein L24	Rpl24	P83732	1.8
60S ribosomal protein L38	Rpl38	P63174	∝
Actin, cytoplasmic	Actb	P60711	∝
ADP-ribosylation factor GTPase-activating protein 2	Arfgap2	Q3MID3	∝
ADP-ribosylation factor GTPase-activating protein 3	Arfgap3	Q4KLN7	∝
Alpha-actinin-1	Actn1	Q9Z1P2	∝
Alpha-crystallin B chain	CRYAB	P05811	∝
Annexin A1	Anxa1	P07150	2.0
AP-2 complex subunit mu	Ap2m1	P84091	2.5
Histone H3.3	H3f3b	P84245	2.2
Ataxin-2	Atxn2	O70305	∝
ATP-dependent RNA helicase DDX3X	Ddx3x	Q62167	2.9
Band 4.1-like protein 5	Epb41l5	Q5FVG2	∝
Calmodulin	Calm1	P62161	2.5
Calmodulin-regulated spectrin-associated protein 2	Camsap2	Q8C1B1	∝
Calponin-1	Cnn1	Q08091	∝
Cdc42 effector protein 1	Cdc42ep1	A1A5P0	∝
Chordin-like protein 1	Chrdl1	Q76LD0	9.0
Cytoplasmic dynein 1 heavy chain 1	Dync1h1	Q9JHU4	1.6
DnaJ homolog subfamily A member 2	Dnaja2	Q9QYJ0	∝
DnaJ homolog subfamily B member 1	Dnajb1	Q9QYJ3	∝
DnaJ homolog subfamily B member 6	Dnajb6	O54946	∝
Elongation factor 1-alpha 1	Eef1a1	P10126	2.0
Elongation factor Tu, mitochondrial	Tufm	P85834	5.0
Filamin-A	Flna	Q8BTM8	1.8

Protein name	Gene name	Accession Number	Fold Change (Syn/Ctrl)
Friend of PRMT1 protein	Fop	Q9CY57	5.0
G kinase-anchoring protein 1	Gkap1	Q5XIG5	3.0
Glial fibrillary acidic protein	Gfap	P47819	3.2
Glutathione peroxidase 1	Gpx1	P04041	2.0
Golgi-associated plant pathogenesis-related protein 1	Glipr2	Q9CYL5	7.0
Heat shock cognate 71 kDa protein	HSPA8	P63018	3.4
Heterogeneous nuclear ribonucleoprotein A1	Hnrnpa1	P04256	∝
Heterogeneous nuclear ribonucleoprotein D0	Hnrnpd	Q60668	∝
Heterogeneous nuclear ribonucleoprotein G retrogene-like	Rbmxrtl	P84586	1.6
Heterogeneous nuclear ribonucleoprotein U-like protein 2	Hnrnpul2	Q00PI9	25.0
Heterogeneous nuclear ribonucleoproteins A2/B1	Hnrnpa2b1	A7VJC2	∝
Histone H1.2	Hist1h1c	P15864	∝
Histone H2A.Z	H2afz	P0C0S6	∝
IQ motif and SEC7 domain-containing protein 1	Iqsec1	Q8R0S2	∝
KH domain-containing, RNA-binding, signal transduction-	Khdrbs1	Q60749	∝
Kinesin-1 heavy chain	Kif5b	Q2PQA9	∝
MAP7 domain-containing protein 1	Map7d1	A2AJI0	∝
Microtubule-associated protein 2	Map2	P15146	5.4
Microtubule-associated protein 4	Map4	Q5M7W5	3.9
Microtubule-associated protein 6	Map6	Q63560	∝
Mitochondrial import inner membrane translocase subunit	Timm44	O35094	∝
Multifunctional protein ADE2	Paics	P51583	3.0
Myosin regulatory light chain 12B	Myl12b	P18666	3.8
Myosin-10	Myh10	Q61879	1.6
Nestin	Nes	P21263	∝
Non-muscle caldesmon	Cald1	Q62736	4.4
Nuclear pore complex protein Nup214	Nup214	Q80U93	∝
Nuclear pore complex protein Nup98-Nup96	Nup98	P49793	∝
PDZ and LIM domain protein 5	Pdlim5	Q62920	19.0
PDZ and LIM domain protein 7	Pdlim7	Q3TJD7	6.0
Pleckstrin homology-like domain family B member 1	Phldb1	Q6PDH0	34.0
Plectin	Plec	P30427	4.8
Pre-B-cell leukemia transcription factor-interacting protein 1	Pbxip1	A2VD12	1.8
Prelamin-A/C	Lmna	P48679	3.3
Protein FAM164A	Fam164a	Q8BJH1	3.0
Protein lin-7 homolog C	Lin7c	O88952	1.7
Ras-related protein Rab-13	Rab13	P35286	∝
Ras-related protein Rab-8B	Rab8b	P61028	∝
Rho-related GTP-binding protein RhoG	Rhog	P84096	∝
Ribosome biogenesis regulatory protein homolog	Rrs1	A1A5P2	3.0
Septin-7	Sept7	O55131	1.8
Serine/arginine repetitive matrix protein 2	Srrm2	Q8BTI8	∝
Serine/threonine-protein kinase DCLK1	Dclk1	Q9JLM8	32.0
Serine/threonine-protein phosphatase PGAM5, mitochondrial	Pgam5	Q562B5	7.0
Serpin H1 (Heat shock protein 47)	Serpinh1	P19324	6.7
Signal recognition particle 54 kDa protein	Srp54	P14576	∝
Sorbin and SH3 domain-containing protein 2	Sorbs2	O35413	∝
Stress-70 protein, mitochondrial	HSPA9	O35501	3.3
Sulfide:quinone oxidoreductase, mitochondrial	Sqrdl	Q9R112	5.5
Trifunctional enzyme subunit alpha, mitochondrial	Hadha	Q64428	4.7
Trifunctional enzyme subunit beta, mitochondrial	Hadhb	Q60587	3.0
Vimentin	Vim	P31000	2.4
Vinexin	Sorbs3	Q9R1Z8	∝
Voltage-dependent anion-selective channel protein 2	Vdac2	P81155	∝

Appendix Table S8

(Data supporting Fig 4B)

Single Particle Tracking of pHluorin-α3-NKA in Presence of ATTO-550-tagged α-Syn

Median Diffusion Coefficient ($\mu m^2/s$)	
Oligomeric α-syn	
OUT	0.11345 (n=1871)
IN	0.0671 (n=394) **(***)**
Fibrillar α-syn	
OUT	0.0995 (n=1305)
IN	0.0704 (n=364) **(***)**

Kolmogorov-Smirnov statistical analysis to test the difference in distribution;
(***p<0.001) n= no of QDs (3-experiments on three independent cultures)

Appendix Table S9

(Data supporting Fig 4D and 4E)

Single Particle Tracking of pHluorin-α3-NKA in Presence of Unlabeled α-syn

(In red: Percentage difference from median value of control)

	No of QDs	Median Diffusion Coefficient ($\mu m^2/s$)		Median Area Explored (μm^2)	
Oligomeric α-syn (SYNAPTIC)					
Control	268	0.0551		0.0884	
Oligomer-5 min	308	0.0440 (**)	-20%	0.0702 (***)	-21%
Oligomer-60 min	306	0.0385 (***)	-30%	0.0602 (***)	-32%
Oligomeric α-syn (EXTRA-SYNAPTIC)					
Control	1273	0.1021		0.2148	
Oligomer-5 min	1277	0.0968 (ns)	-5%	0.2028 (*)	-6%
Oligomer-60 min	1360	0.0823 (***)	-19%	0.1679 (***)	-22%
Fibrillar α-syn (SYNAPTIC)					
Control	373	0.0603		0.0917	
Fibril-5 min	528	0.0546 (*)	-9%	0.0668 (***)	-27%
Fibril-60 min	466	0.0476 (***)	-21%	0.0641 (***)	-30%
Fibrillar α-syn (EXTRA-SYNAPTIC)					
Control	1234	0.0925		0.1631	
Fibril-5 min	1484	0.0694 (***)	-25%	0.1228 (***)	-24%
Fibril-60 min	1520	0.0583 (***)	-36%	0.1010 (***)	-38%

Kolmogorov-Smirnov test to compare difference in distribution relative to "Control"

ns = not significant, *p<0.05; **p<0.01; ***p<0.001

4-experiment each for oligomeric and fibrillar α-syn was performed on independent cultures and on separate days.

Appendix Table S10

(Data supporting Fig 6B)

Enrichment of α3-NKA over α-Syn at Synapses

	Fluorescence Intensity of α3-NKA clusters Normalized to Control-synaptic (Mean ± SEM)	
	Synaptic	**Extra-Synaptic**
Control	1.00 ± 0.06 (n=60)	0.38 ± 0.02 (n=60)
Oligomer-5 min	1.22 ± 0.06 (n=60) **(**)**	0.42 ± 0.02 (n=60) **(ns)**
Oligomer-60 min	1.25 ± 0.09 (n=60) **(**)**	0.39 ± 0.01 (n=60) **(ns)**
Fibril-5 min	1.18 ± 0.05 (n=60) **(*)**	0.41 ± 0.01 (n=60) **(ns)**
Fibril-60 min	1.42 ± 0.07 (n=60) **(***)**	0.48 ± 0.02 (n=60) **(ns)**

One-way ANOVA with Dunnett's test to compare the difference from control

ns = not significant, *p<0.05; **p<0.01; ***p<0.001

n = field of view; (3-experiments on three independent cultures)

MATERIAL AND METHODS

Preparation, labeling, characterization and assembly of α-syn

Recombinant wild type (WT) and C-terminally S-tagged (α-syn-S-tag) human α-syn were expressed and purified as described previously (Ghee et al, 2005). α-syn concentration was determined spectrophotometrically using an extinction coefficient of 5960 $M^{-1}cm^{-1}$ at 280 nm. Pure monomeric α-syn (0.2–0.5 mM) in 50 mM Tris–HCl, pH 7.5, 150 mM KCl (buffer A) was filtered through sterile 0.22 µm filters and stored at -80 °C. For oligomers and fibrils formation, monomeric α-syn in buffer A were respectively incubated at 4°C for 7 days or 37°C for 4 days under continuous shaking in a thermomixer (Eppendorf, Germany) set at 600 rpm, respectively. Assembly into fibrils was monitored using Thioflavin T binding. Aliquots (10 µl) were withdrawn at different time intervals from the assembly reaction and mixed with 400 µl of Thioflavin T (10 µM) in water and Thioflavin T fluorescence (Excitation wavelength: 440 nm and emissions wavelengths: 480 nm) was recorded using a Cary Eclipse Spectrofluorometer (Varian Inc., Palo Alto, USA). Oligomeric α-syn was separated from monomeric α-syn by size exclusion chromatography using a Superose®6 HR10/30 column (GE Healthcare) equilibrated in phosphate buffered saline (PBS) buffer. Fibrillar α-syn was separated from monomeric α-syn through 2-cycles of sedimentation at 15000g and re-suspension of the pellet (**Appendix Figure S1**).

Oligomeric or fibrillar α-syn in PBS were labeled by addition of 2 molar excess of the aminoreactive fluorescent dye ATTO-550 (Reference: AD 550-35, ATTO-Tech GmbH) or biotin using EZ-link Sulfo-NHS-Biotin (sulfosuccinimidobiotin, Perbio Science, UK). Labeling was performed following the manufacturer's recommendations. Unreacted dye or biotin were removed by size exclusion chromatography or three cycles of sedimentation and suspension in PBS for oligomeric or fibrillar α-syn, respectively. The amount of incorporated ATTO 550 and biotin was assessed by mass spectrometry (**Appendix Figure S1**). The samples were de-salted (with 5% acetonitrile, 0.1% Trifluoroacetic acid (TFA)) and eluted from a C18 reversed-phase Zip-Tip (Millipore, Billerica, MA, USA) in 50% acetonitrile, 0.1% TFA. Peptide samples were mixed in a ratio of 1:5 to 1:20 (v/v) with sinapinic acid (10 mg/mL) in 50% acetonitrile and 0.1% TFA) and spotted (0.5 µL) on a stainless steel MALDI target (Opti-TOF; Applied BioSystems). MALDI-TOF-TOF MS spectra were acquired with a MALDI-TOF/TOF 5800 mass spectrometer (Applied Biosystems) using linear mode acquisition. External calibration was performed using unmodified WT α-syn. Acquisition and data analysis were performed using the Data Explorer software from Applied Biosystems.

The nature of all α-syn assemblies used was routinely assessed using a Jeol 1400 (Jeol Ltd., Peabody, MA) Transmission Electron Microscope (TEM) after adsorption of the samples onto carbon-coated 200-mesh grids and negative staining with 1% uranyl acetate. The images were acquired with a Gatan Orius CCD camera (Gatan). The particle concentration of oligomeric and fibrillar α-syn samples was assessed by analytical ultracentrifugation (AUC) and quantitative transmission electron microscopy (TEM) as previously

described (Pieri et al, 2012). The particle concentration of α-syn (tagged and untagged) was obtained by dividing α-syn monomeric concentration by the average number of molecules (as measured by AUC and TEM). For our preparation, the average number of molecules measured for oligomeric and fibrillar α-syn was 40 and 8333, respectively. The concentration of oligomeric α-syn was 25 nM and that of fibrillar α-syn was 0.03 nM, unless specified, corresponding to 1 μM or 0.25 μM monomeric α-syn, respectively.

Aβ-oligomers preparation, purification and characterization has been recently described in Shrivastava et al, 2013a.

Primary neuronal cultures

All cultures were prepared from 18-day-old Sprague-Dawley rat embryos (Janvier Labs, France). Pull down and proteomics studies were performed on pure cultures of rat cortical neurons plated on 10 cm plates pre-coated with 80 mg/ml poly-D, L-ornithine. Cortical neurons were used, as they can be prepared in larger quantities (4 X 10^6 cells/dish) as required for these experiments. Pure neuronal cultures were maintained in astrocyte-conditioned neuronal medium supplemented with cytosine-arabinoside (5 μM) as has been recently described (Shrivastava et al, 2013a). All other experiments were performed on rat striatal neuronal cultures plated on 18 mm coverslips pre-coated with 80 mg/ml poly-D, L-ornithine (Renner et al, 2010). Freshly dissociated (trypsin) striatal cells were plated (10^5 cells/well) in neuronal attachment media consisting of 10% horse serum, 1 mM sodium pyruvate, and 2 mM glutamine in MEM for 3 h. The attachment medium was replaced and cells were maintained in serum-free neurobasal medium supplemented with B27 (1X) and glutamine (2 mM). After 2 days, culture medium was supplemented with cytosine-arabinoside to restrict the growth of astrocytes. Cells were maintained by supplementing with fresh medium every week.

Pull-down of α-syn-S-tag bound protein complexes and sample preparation for mass spectrometry (MS)

Oligomeric or fibrillar α-syn-S-tag (40 μM monomer concentration) were added to the culture medium of 2 weeks old pure cortical neuron cultures of rat (3-4 culture dishes per condition). Unexposed neurons were used as control. After 10 minutes, cells were washed twice with 1X PBS and scraped on ice in 50 mM Hepes-KOH (pH 7.5), 2 mM EDTA, 0.1% Triton X-100, supplemented with complete protease inhibitor cocktail (Roche). The extracts were flash frozen in liquid nitrogen and stored at -80°C. Cell lysis was completed by sonication and the protein concentration in the extracts determined using BCA assay kit (Thermo Scientific). To pull down oligomeric or fibrillar α-syn-S-tag together with their specific protein partners, 0.5 mg of total protein extracts were incubated with S-protein agarose (200 μl settled resin) (Novagen) equilibrated in 500 μl binding buffer (20 mM Tris-HCl pH 7.5, 150 mM NaCl, 0.1% Triton X-100, Complete protease inhibitors) for 1 h at 4 °C under gentle agitation. Extracts from control-unexposed neurons were also incubated with S-protein agarose beads and used as control. After 3 washes with 5 ml

binding buffer and 3 washes with 5 ml Triton-free binding buffer, the resin was re-suspended in 400 µl of 50 mM ammonium bicarbonate pH 8 in the presence of 0.1% RapiGest (Waters corporation, Milford, MA) and heated at 95°C for 10 min. Proteins were then reduced in the presence of 10 mM dithiotreitol (DTT) at 56°C for 30 min and alkylated in 20 mM iodoacetamide (Sigma) at room temperature in the dark for 45 min. Proteins bound to the S-protein agarose beads were digested on the resin by incubating the samples overnight at 37 °C in the presence of 0.8 µg trypsin Promega Gold (Promega, Madison, WI). After digestion, the samples were centrifuged for 10 min at 16000g to discard the resins. Trypsin digestion and RapiGest treatment in the supernatants were stopped by addition of 0.5% TFA and incubation at 37°C for 45 min. The tryptic peptide samples were spun for 10 min at 16000g and the supernatants were stored at -80°C for MS analysis.

In the experiments where the cross-linker DTSSP was used to cross-link fibrillar α-syn-S-tag to its partner membrane proteins, 2 weeks old cortical neurons were treated for 30 minutes with chondroitinase (0.02u/ml) prior to the addition of fibrillar α-syn-S-tag to favor the interactions. Chemical cross-linking with DTSSP (1 mM in PBS, Pierce, Waltham, MA)) was carried out for 30 min at room temperature prior to cell scraping and pull-down of α-syn-S-tag cross-linked proteins. For MS identification of α-syn cross-linked proteins further treatment and protein digestion was performed as described above. For the α3-NKA peptide targeted identification strategy, the nanoLC-MS/MS data were processed automatically using the Thermo Proteome Discoverer software (version 1.4) and the SEQUEST search engine with α3-NKA primary structure and the following chemical modifications: cysteine carbamidomethylation as fixed modification and methionine oxidation, N-terminal acetylation, and monolink modification of K, S, Y and T residues with DTSSP as variable modifications.

Mass spectrometric identification and quantification of the pulled-down proteins

For each pull down, 15 µl of tryptic peptide digests were analyzed by nanoLC-MS/MS using an EASY-nLC II high performance liquid chromatography (HPLC) system (Proxeon, Thermo- Scientific, Waltham, MA) coupled to the nanoelectrospray ion source of a Linear Ion Trap-OrbitrapVelos mass spectrometer (Thermo Scientific). Peptide separation was performed on a reversed phase C18 nano HPLC column (100 µm inner diameter, 5 µm C18 particles, 15 cm length, NTCC-360/100-5) from Nikkyo Technos (Nikkyo Technos Co., Ltd., Tokyo, Japan). The peptides were loaded at a pressure-dependent flow rate corresponding to a maximum pressure of 200 bars and eluted at a flow rate of 300 nl/min using a two slope gradient of first 5 to 20% solvent B for 60 min, followed by 20 to 40% solvent B in 40 min and a washing step at 100% solvent B. Solvent A was 0.1% formic acid in water, and solvent B was 0.1% formic acid in 100% acetonitrile. NanoLC-MS/MS experiments were conducted in the data-dependent acquisition mode. The mass of the precursors was measured with a high resolution (60,000 full weight at half maximum) in the Orbitrap. The 20 most intense ions, above an intensity threshold of 5000 counts, were selected for CID fragmentation and

analysis in the LTQ. NanoLC-MS/MS data were processed automatically using the Scaffold software (version 3.6.4) and the SwissProt_18112011 database with both the Mascot (Perkins et al., 1999) (Version: 2.3.02) and the X! Tandem (Craig & Beavis, 2004) (Version CYCLONE 2010.12.01.1) search engine, a specific trypsin digestion with up to 2 missed cleavages, a tolerance of 0.5 Da for fragment monoisotopic masses and 6 ppm for parent monoisotopic mass tolerance, and the following chemical modifications: Carbamidomethylation of Cys as fixed modification, and dehydration, ammonia loss, oxidation of methionine and N-acetylation as variable modifications. For the Scaffold analysis, thresholds were set at 90% minimum for peptides and 99% and 2 unique peptides minimum for protein.

Identified proteins were quantified by a label-free proteomic approach using spectral counting (Liu et al, 2004) with the Scaffold software. Comparison between controls and samples identified some proteins as 60S ribosomal proteins, nucleolin and ribonuclease inhibitor as major contaminants. Among them nucleolin presented the best reproducibility among experiments and was chosen to normalize the spectral counting data. Only proteins identified with at least 2 unique peptides in at least 2 replicates were quantified. Only proteins with a spectral count ratio, between the cells exposed to α-syn (either oligomeric or fibrillar) and the control cells, above 1.6 and a p-value <0.05 were considered as significantly increased in the pull-down and thus considered as α-syn interacting proteins. Spectral count ratios presented in **Appendix Table S5-6** were calculated from averaged spectral counts of three independent replicates. Finally the membrane protein annotation was obtained using the NCBI annotation tool of the Scaffold software. For proteins annotated as membrane proteins, including peripheral extracellular or intracellular membrane proteins and integral membrane proteins, validation of the membrane localization was performed with data reported in the literature (see validated membrane protein list in **Appendix Table S5-6**).

Co-immunoprecipitation of α3-NKA and α-syn

Total protein extracts (1.5 mg in in RIPA buffer, 50 mM Tris-HCl pH 7.5, 50 mM NaCl, 2 mM EDTA, 0.5 mM sodium deoxycholate, 0.5% NP-40%, Complete protease inhibitors) were pre-incubated with protein A sepharose (GE Healthcare) for 1h at 4°C. The supernatant was incubated with Goat polyclonal anti Na+/K+ -ATPase alpha3 (C-16, Santa Cruz Catalogue # sc-16052) (5 µg) overnight at 4 °C under gentle agitation. Samples were then incubated with protein A-sepharose beads (100 µl settled resin) (GE-Healthcare) for 1 h at 4 °C under gentle agitation. As a negative control, protein extracts were incubated with protein A-sepharose beads in the presence of pre-immune goat IgGs. After incubation, the beads were washed with RIPA buffer. The protein A-bound protein complex were denatured with SDS-PAGE buffer for 5 min at 95 °C, resolved on 10% polyacrylamide gels and probed with anti α-syn (1:2000, BD Biosciences Cat # 610787) antibody. Blots were stripped (2h, heating at 50°C in 62.5 mM Tris HCl pH 6.8, 2% SDS, 100 mM beta-mercaptoethanol) and re-probed with an anti α-tubulin (1:4000, Abcam mouse monoclonal, DM1A, Cat # ab7291) antibody.

In vivo injection of α-syn assemblies and tissue preparation

Sprague-Dawley rats were obtained from Janvier Labs, France and maintained at the animal house facility (École Normale Supérieure) until surgery. Oligomeric or fibrillar α-syn injection was performed in 10-week old rats (1 male and 1 female for each α-syn subtype). Following anesthesia (106 mg/kg ketamine and 7.5 mg/kg xylazine), animals were placed on a stereotaxis apparatus. A tiny hole in the skull was opened and 5 µl of α-syn (oligomer: 100 µM, fibril: 20 µM monomer concentration) were pressure-injected at a depth of 4.5 mm in the striatum at a flow rate of 0.5 µl/min (from the bregma: anteroposterior (AP) 0mm, mediolateral (ML) +3 mm, dorsoventral (DV) +4.5 mm). 8 hr (oligomeric) or 24 hr (fibrillar) following injection, animals were anesthetized using 80 mg/kg pentobarbital intra peritoneal and trans-cardially perfused with 4% paraformaldehyde. Their brains were collected and cryo-protected using sucrose before sectioning. 30 µm thick coronal sections were prepared using cryostat maintained at -20ºC. Brain sections were stored in 1X PBS-sodium azide solution and immunohistochemistry performed within 10 days.

Immunohistochemistry, immunocytochemistry and image acquisition and quantification

Brain sections were extensively washed in 1X PBS to remove azide followed by blocking in 0.1% gelatin and 0.2% Triton-X-100 in 1X PBS for 45 min. Sections were then incubated overnight with the appropriate primary antibodies diluted in PBS: Rabbit-Homer (1:1000, Synaptic System), Mouse Gephyrin (1:1000, Synaptic System), Mouse MAP2 (1:1500, Millipore), Mouse-α3-NKA (XVIF9-G10) (1:1000, Thermo Scientific), Rabbit-Synapsin (1:1500, Synaptic System). Following 3 washes (20 min each), slices were incubated with appropriate secondary antibodies (FITC or cy5 conjugated; 1:500, 3 hr). After washing for 2 hr, sections were mounted onto glass slides using Vectashield (Vector Labs). Nuclear stain (DAPI) was added in the mounting medium (1:400). Images were acquired using a Leica confocal TCS SP5 microscope and processed using ImageJ and Metamorph (Molecular Devices) software. For each animal, staining was performed in randomly chosen 5-6 sections within ±250 µm from the site of injection. In addition images were acquired from nearly 8-10 randomly chosen regions within the striatum.

Immunocytochemistry was performed as per standard protocol and used previously (Shrivastava et al, 2013a). Permeabilization was performed before antibody incubation as antibody against α3-NKA has intracellular epitope. Even after permeabilization, α3-NKA immunoreactivity was pre-dominantly found on the plasma membrane as observed previously (Azarias et al, 2013). Following primary antibody incubation for 1 hr: Rabbit-Homer (1:400, Synaptic System), Mouse-Gephyrin (1:400, Synaptic System), Mouse-α3-NKA (1:3000, Thermo Scientific), Rabbit-Synapsin (1:800, Synaptic System), Rabbit Tau (1:400, Synaptic System), Mouse MAP2 (1:400, Millipore). For α-syn staining, no permeabilization was performed and mouse monoclonal antibody was used (Clone 42/α-syn; BD Bioscience). Images were acquired using Leica Inverted Spinning Disk microscope (DM5000B, Coolsnap HQ2 camera, Cobolt lasers).

Confocal and spinning disk images were filtered by wavelet decomposition using an interface implemented in Metamorph (Racine et al, 2007). Wavelet decomposition allows the separation of small and large structures (clusters) based on their fluorescence intensities. This approach was used to generate background free masks showing sites that are enriched (cluster) with a specific protein of interest (homer/gephyrin/synapsin/α3-NKA) and has been used in previous publications (Bannai et al, 2009; Renner et al, 2010; Shrivastava et al, 2013a). "Intensity of cluster" means total fluorescence intensity per cluster. Co-localization and/or apposition between the clusters of two images were determined using the masks using Matlab where the total fluorescence intensity of clusters was quantified on the original images after identifying the clusters that were totally or partially co-localizing on the masks (Renner et al, 2010; Shrivastava et al, 2013a). No of fields" in the figure legend refer to the number of microscopic field (1392 x 1042 pixel) that were quantified. Intensity Correlation Quotient (ICQ) was computed on entire field of view using plugin in ImageJ as per the instructions (Li et al, 2004).

Plasmids and Transfection

TMR-Dendra construct was prepared by replacing GFP with Dendra fluorescent protein (Ribrault et al, 2011). Extracellular pHluorin-tagged α3-NKA and extracellular EGFP-tagged β1-NKA plasmids were generated and characterized by Thomas Liebmann. pHluorin was inserted in the 2nd extracellular loop between Trp^{307} and Leu^{308} (Rat sequence: NP_036638). Chimeric α3/α1-NKA-a, b and c were generated using site-directed mutagenesis kit (Agilent). Transfection was performed using lipofectamine-2000 (Invitrogen). Transfection medium (TM) was composed of 1 mM sodium pyruvate and 2 mM glutamine in nerobasal medium (Invitrogen). 0.5 µg of plasmid and 2 µl of lipofectamine-2000 reagent were added separately in 50 µl of TM. After 10 min, the two solutions were mixed and left for another 15 min at room temperature. During this period, culture medium from cells was replaced with pre-warmed TM. The culture medium was stored at 37ºC. 100 µl of Lipofectamine-plasmid mix was then added on top of cells. After 30 min, cells were washed with TM and replaced with original culture medium.

Single particle tracking and analysis

Quantum dot (QD) based single particle tracking (SPT) protocol and analysis methods have been used and described in several previous publications (Renner et al, 2010, Shrivastava et al, 2013a). For all experiments, α-syn exposure was performed on live neurons in the culture medium and in an incubator maintained at 37ºC/5%CO_2. Unbound α-syn was washed before experiments. All the washing and imaging was performed in MEM recording medium (Phenol red-free MEM, 33 mM glucose, 20 mM HEPES, 2 mM glutamine, 1 mM sodium pyruvate, and 1X B27). For SPT of α-syn, biotin labeled α-syn assemblies were used. Following exposure to α-syn assemblies, cells were incubated with streptavidin-QD-605nm (1:5000, 2 min). For SPT of α3-NKA, cells were transfected with pHluorin-tagged α3-NKA plasmid. Neurons were

labeled using GFP-antibody pre-coupled with QD-605 nm (pre-coupling protocol: 1 µl rabbit-GFP antibody + 1 µl $F_{ab'}$-QD-605 + 7 µl 1X PBS, mix and gently shake for 30 min, add 1 µl 1X casein and shake for additional 15 min) (Renner et al, 2009). Synapses were labeled and identified using FM4-64 labeling. All SPT-experiments were performed on neurons aged DIV 16-17. Transfection was preformed on DIV 14. Tracking and analysis was performed using SPTrack_v4, homemade software in Matlab (MathWorks) (Renner et al, 2010). The center of the QD fluorescence spot was determined by Gaussian fit with a spatial resolution of 10–20 nm. The spots in a given frame were associated with the maximum likely trajectories estimated on previous frames of the image sequence. Trajectories with a minimum length of 15 consecutive frames were used. The mean square displacement (MSD) was calculated using $MSD(ndt) = (N - n)^{-1} \Sigma_{i=1}^{N-n} [(x_{i+n} - x_i)^2 + (y^{i+n} - y_i)^2]$, where x_i and y_i are the coordinates of an object on frame I, N is the total number of steps in the trajectory, dt is the time between two successive frames, and ndt is the time interval over which displacement is averaged (Saxton and Jacobson, 1997; Triller and Choquet, 2008). The diffusion coefficient D was calculated by fitting the first two to five points of the MSD plot versus time with the equation $MSD(t) = 4D_{2\text{-}5t} + 4\sigma^2_x$, with σ_x is the spot localization accuracy in one direction. Explored area represents the distribution of MSD values at a given interval of time. The explored area of individual trajectories was calculated as the area covered by trajectory in μm^2 during a time-interval of 600 ms to 900 ms. Analysis of the explored area reveals the heterogeneity of the diffusion in the population of trajectories and allows applying statistical tests on MSD data.

Super-resolution STORM imaging and analysis

Stochastic Optical Reconstruction Microscopy (STORM) imaging, buffer composition and analysis was recently described (Specht et al, 2013; Shrivastava et al, 2013b). STORM was performed following immunolabeling of α3-NKA (Mouse-α3-NKA, 1:3000, 1 hr). Alexa Fluor 647-conjugated (Invitrogen) secondary antibodies were used. Imaging (Alexa647 alone or Alexa647/Dendra) was performed under reducing condition with buffer composed of PBS (pH 7.4), glucose (10%), β-mercaptoethylamine (50 mM), glucose oxidase (0.5 mg/ml), and catalase (40 mg/ml), and degassed with N_2 (Specht et al, 2013). For 2-color STORM involving ATTO488 dye, 10 mM β-mercaptoethylamine was used (Dempsey et al, 2011). STORM imaging was carried out on an inverted Nikon Eclipse Ti microscope equipped with a 100X oil-immersion objective (N.A. 1.49 with a microscope-inbuilt 1.5X lens) using an Andor iXon EMCCD camera (image pixel size, 107 nm). Alexa fluor 647 was imaged using laser 639 nm (1 kW, used at 500 mW) for a 50 ms exposure time. A low-wavelength laser (532 nm (0.5 kW), used at 25-75 mW) was used to convert Alexa fluor 647 from off to on state. TMD-Dendra was imaged using laser 561 nm (0.5kW, used at 300mW) while activating with 405 nm laser (100 mW power, used at 1-10 mW). ATTO488 was imaged with 488 nm laser (0.5kW, used at 75-100 mW) and activated using 405 nm laser. Single molecules detection and rendering was recently described (Shrivastava et al, 2013b). For α3-NKA-Alexa647 quantification, individual detections were rendered using a pixel size of 5 nm and Gaussian of 10 nm to visualize clusters

and separate closely spaced clusters. This intensity-based render images were then thresholded using ImageJ to isolate clusters of α3-NKA. The threshold-images were then masked on top on individual detections to compute number of detections per cluster. Distance between clusters measures the separation between the centroid of two nanoclusters of α3-NKA. This was measured within a maximum radius of 300 nm from the centroid of a given nanocluster. For α-syn-Alexa647, TMD-Dendra and α3-NKA visualization, rendering was done with a pixel size of 20 nm and Gaussian radius of 10 nm.

An implementation of the DBSCAN (Density-Based Spatial Clustering of Applications with Noise) algorithm (Ester et al, 1996) was used for the density based clustering of α3-NKA detections. This approach can identify clusters in large spatial data sets by looking at the local density of points. A lowest 'density threshold' of minimum 5 detections within a radial distance of 500 nm was used. Higher thresholds used decreasing radial distances. Detections below local 'density threshold' or threshold distance were considered non-clustered.

Tetraspeck^{TM} microsphere multicolor beads (0.1µm, Invitrogen, T7279) were used for all STORM imaging experiments to correct for stage drift and 2-color-alignment (for 2-color STORM). Beads were diluted to 1:200 (in 1X PBS) and applied for 2 min before imaging. Unbound beads were washed extensively (~10-12 washed). Stage drift (x/y) was corrected over sliding window of 1000 frames (Specht et al, 2013; Shrivastava et al, 2013b). For 2-color STORM images, positions of at least 2-3 beads were simultaneously aligned using ImageJ to ensure correct alignment of two channels.

Sodium Dye Loading, Imaging and Analysis

Recordings were performed on primary striatal cultures on day *in vitro* 16–21. Cells exposed or not to α-syn assemblies were loaded with the acetoxymethyl ester derivative forms of the Na^+ sensitive cytosolic ANG2 (Asante NaTRIUM Green 2; 37°C, 5% $C0_2$) at 5 µM for 30 min in the cell culture medium (Neurobasal, 2% B27, 0.25% L-Glutamine). After washing, the coverslips were placed on a hot plate maintained at 37°C for 20 min in "recording solution" (110 mM NaCl, 4 mM KCl, 1.5 mM $CaCl_2$, 1.2 mM $MgSO_4$, 25 mM $NaHCO_3$, 1 mM NaH_2PO_4, 20 mM HEPES, 10 mM glucose, pH 7.4). For imaging, coverslips were mounted on a heated chamber attached with perfusion system for rapid exchange of solutions. ANG2 fluorescence was excited at 490 nm and collected above 500 nm, using a Zeiss Axioscope Observer D1 equipped with a 40X, 1.3NA oil objective and an Andor Ixon camera. The K^+ free recording solution (~25 ml, 0 mM K^+) had the same composition, except that the NaCl and KCl concentrations were 114 mM and 0 mM, respectively. The 0 mM K^+ recording solution was replaced with normal recording solution and recovery to basal level was monitored until a plateau was reached. At the end of each experiment, neurons were super-fused with Na^+ calibration solutions containing stepwise increasing concentrations of Na^+ in the presence of 3 µM gramicidin, 10 µM monensin, and 1 mM ouabain until a plateau was reached (**Appendix Figure S6**). Na^+

calibration solutions contained [Na^+ + K^+] = 165 mM, 136 mM gluconate, 1.2 mM $MgSO_4$, 0.78 mM KH_2PO_4, 20 mM HEPES, 1.3 mM $CaCl_2$, pH adjusted to 7.2 with KOH.

In each experiment, 8-10 regions of interest (ROI) were selected around primary or secondary dendrites from 3-5 cells (using ImageJ). The fluorescence levels for each ROI were measured against time. The Na^+ data were then analyzed using custom-written code in MATLAB (MathWorks). The fluorescence (F) was corrected for bleaching, smoothed using a 7-point moving average, and normalized to the fluorescence levels of the calibration solutions containing 10mM Na^+ (F_{10mM}). The increase in peak was defined as F/F_{10mM}(peak) – F/F_{10mM}(baseline). The recovery to basal was defined as [F/F_{10mM}(peak) – F/F_{10mM}(plateau after the peak)]/ [F/F_{10mM}(peak) – F/F_{10mM}(baseline)]x100 (See pictorial representation in **Appendix Figure S6**). The Na^+ extrusion rate was quantified by fitting the recovery slope to a bi-exponential equation. The apparent maximum initial pumping rate was taken as the absolute value of the maximum derivative of the fitted function.

Calcium Imaging and Analysis

Ca^{2+} imaging was performed following Fluo-4 (1 μM) labeling of neurons for 5 min at 37ºC in MEM recording medium as previously (Renner et al, 2010). After final wash, cells were allowed to recover for 5-10 min before imaging. Images were acquired on an inverted spinning disk microscope (Nikon Eclipse Ti with Yokogawa spinning disk) at 10X magnification using a 491 nm wavelength laser (100 mW, Cobolt Calypso). Imaging was performed in a controlled environment at 37ºC and 5% CO2. Time-lapse images were acquired at 0.2 Hz at 50% laser power and 50 ms exposure time to minimize photo-toxicity. Glutamate (100 μM final concentration) was manually applied using a pipette. For quantification, regions of interest were selected on cell body and total-fluorescence intensity was determined on background-subtracted images (ImageJ). For statistical analysis, ratio of change in fluorescence following glutamate application was calculated. The ratio represents the average intensity of 5 images recoded after glutamate addition divided by the average of 5-images obtained before glutamate application.

Software and Statistics

All analysis of immunocytochemistry, immunohistochemistry, SPT, Na^+ imaging and STORM were processed and analyzed on MATLAB (Mathworks). Microsoft Excel, Adobe Illustrator, ImageJ and Graph Pad Prism were used for the preparation of figures. The statistical test used is mentioned in figure legends (and supplementary tables). For SPT, Kolmogorov-Smirnov test was used to test the differences in distribution. Pooled diffusion coefficient values from multiple experiments were used as in previous studies (Bannai et al, 2009; Renner et al, 2009, Renner et al, 2010; Shrivastava et al, 2013a, b).

SUPPLEMENTAL REFERENCES

Bannai H, Lévi S, Schweizer C, Inoue T, Launey T, Racine V, Sibarita JB, Mikoshiba K, Triller A (2009) Activity-dependent tuning of inhibitory neurotransmission based on $GABA_AR$ diffusion dynamics. Neuron 62: 670–682

Craig R, Beavis RC (2004) TANDEM: matching proteins with tandem mass spectra. Bioinforma 20: 1466–1467

Dempsey GT, Vaughan JC, Chen KH, Bates M, Zhuang X (2011) Evaluation of fluorophores for optimal performance in localization-based super-resolution imaging. Nat Methods 8: 1027-1036

Ghee M, Melki R, Michot N, Mallet J (2005) PA700, the regulatory complex of the 26S proteasome, interferes with alpha-synuclein assembly. FEBS J 272: 4023–4033

Liu H, Sadygov RG, Yates JR 3rd (2004) A model for random sampling and estimation of relative protein abundance in shotgun proteomics. Anal Chem 76: 4193–4201

Perkins DN, Pappin DJ, Creasy DM, Cottrell JS (1999) Probability-based protein identification by searching sequence databases using mass spectrometry data. Electrophoresis 20: 3551–3567

Racine V, Sachse M, Salamero J, Fraisier V, Trubuil A, Sibarita, JB (2007) Visualization and quantification of vesicle trafficking on a three-dimensional cytoskeleton network in living cells. J Microsc 225: 214-228

Shrivastava AN, Kowalewski JM, Renner M, Bousset L, Koulakoff A, Melki R, Giaume C, Triller A (2013a) β-amyloid and ATP-induced diffusional trapping of astrocyte and neuronal metabotropic glutamate type-5 receptors. Glia 61: 1673–1686

Shrivastava AN, Rodriguez PC, Triller A, Renner M (2013b) Dynamic micro-organization of P2X7 receptors revealed by PALM based single particle tracking. Front Cell Neurosci 7: 232

Specht CG, Izeddin I, Rodriguez PC, El Beheiry M, Rostaing P, Darzacq X, Dahan M, Triller A (2013) Quantitative Nanoscopy of Inhibitory Synapses: Counting Gephyrin Molecules and Receptor Binding Sites. Neuron 79: 308-321.